RAPID COMMUNICATIONS

PHYSICAL REVIEW B VOLUME 44, NUMBER 11 15 SEPTEMBER 1991-I

Electroreflectance detection of resonant coupling between Wannier-Stark localization states in a GaAs/AlAs superlattice

M. Nakayama, I. Tanaka, and H. Nishimura
Department of Applied Physics, Faculty of Engineering, Osaka City University, Sugimoto, Sumiyoshi-ku, Osaka 558, Japan

K. Kawashima and K. Fujiwara
ATR Radio Communications Research Laboratories, Seika-cho, Soraku-gun, Kyoto 619-02, Japan
(Received 17 May 1991; revised manuscript received 9 July 1991)

We report electroreflectance (ER) detection of the resonant coupling between the Wannier-Stark localization states in a GaAs(6.4 nm)/AlAs(0.9 nm) superlattice. We find that the ER line shapes of the heavy-hole and light-hole exciton transitions associated with the first ($n=1$) subbands clearly exhibit splitting features with anticrossing behaviors, resulting from the second- and third-nearest-neighbor resonant couplings between the $n=1$ and $n=2$ electron subbands, and that the intensities are remarkably reduced in the resonant condition owing to the delocalization of the electron wave function. In addition, it is demonstrated that ER spectroscopy is much more sensitive to detect the resonant coupling than photocurrent spectroscopy. We analyze the ER results of the resonant coupling by using a transfer-matrix method with Airy functions.

In the last few years, there has been a considerable interest in spatial localization of extended miniband states induced by an electric field F, Wannier-Stark (WS) localization, in a semiconductor superlattice (SL).[1-11] The WS localization leads to Stark-ladder transitions: E_0+veFD ($v=0,\pm1,\pm2,\ldots$), where E_0 is an interband transition energy in an isolated quantum well (QW), D is a SL period, and v is a Stark-ladder index indicating an oblique transition in real space. If the energy of $veFD$ just agrees with the energy spacing between the $n=1$ electron subband and the $n=2$ subband, it is expected that the WS localization state of the $n=1$ subband in a QW resonantly couples with that of the $n=2$ subband in the vth nearest-neighbor QW, and that the resonant coupling causes the delocalization of the localized wave function. This is an interesting high-electric-field effect on SL electronic properties. Very recently, Schneider *et al.* reported such a phenomenon in a GaAs/AlAs SL observed by using photocurrent (PC) spectroscopy.[9]

In the present work, we have detected the resonant coupling between the WS localization states of the electron subbands in a GaAs(6.4 nm)/AlAs(0.9 nm) SL by using electroreflectance (ER) spectroscopy. In addition, we have measured PC spectra to compare them with the ER spectra. Until now, PC spectroscopy has been a major method for investigating WS localization. In our previous work[11] and Ref. 10 it has been revealed that ER spectroscopy is highly sensitive to Stark-ladder transitions compared with PC spectroscopy. In Ref. 9, the first- and second-nearest-neighbor resonant couplings between the WS localization states are discussed on the basis of the PC spectra. The second-nearest-neighbor resonant coupling is not directly observed in the PC spectra, but the coupling is estimated from I-V curves at various photon energies of the heavy-hole exciton transition. In this paper we report that the ER line shapes of the heavy-hole and light-hole exciton transitions associated with the $n=1$ subband states clearly exhibit splitting features with anticrossing behaviors, resulting from the second- and third-nearest-neighbor resonant couplings. We analyze the ER results of the resonant coupling by using a transfer-matrix (TM) method.[12]

The sample used in this work was grown on a n-type (Si-doped) (001)-GaAs substrate by molecular-beam epitaxy. The GaAs(6.4 nm)/AlAs(0.9 nm) SL has 20 periods and is placed in the center of a p-i-n diode structure, where the n and p layers are Si-doped (1×10^{18} cm^{-3}) and Be-doped (1×10^{19} cm^{-3}) $Al_{0.33}Ga_{0.67}As$ layers with 0.8 μm thickness, respectively. The layer thickness of the SL was deduced from the calibrated growth rate, and the SL period was determined to be 7.39 nm by small-angle x-ray-diffraction method.[6] The sample was processed into a mesa structure with $\sim$200 μm diameter. The method for making an Ohmic contact is described in Ref. 6. The ER and PC measurements were performed at 77 K. The probe light was produced by combination of a halogen lamp (50 W) and a single monochromator (32-cm focal length) with 0.5-nm resolution. The reflected light was detected with a Si photodiode. In the ER measurements, the electric field was modulated with the amplitude of 25 mV and the frequency of 210 Hz around a given dc bias. The ER signals were obtained by a conventional lock-in technique. The PC signals were measured with a picoammeter.

First we compare the systematic experimental results of the Stark-ladder transitions with the calculated results by the TM method. Figure 1 shows the ER (ΔR) and PC spectra of the GaAs(6.4 nm)/AlAs(0.9 nm) SL at 77 K in the energy range of the heavy-hole and light-hole exciton transitions associated with the $n=1$ subbands, where the dashed curves indicate the magnified spectra, and the value of the electric field in the parentheses is estimated from the built-in voltage of 1.64 V. The ER spectra are not normalized by reflectance (R) because the surface Ohmic electrode prevents the obtainment of the real R signal from the SL. The PC spectra exhibit two exciton-

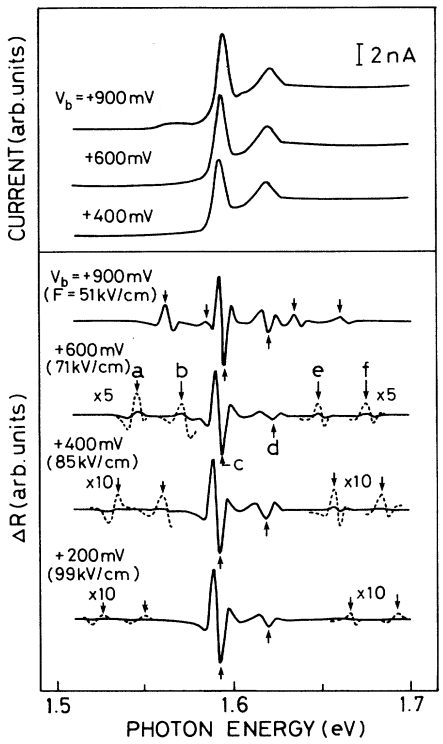

FIG. 1. Electroreflectance and photocurrent spectra of the GaAs(6.4 nm)/AlAs(0.9 nm) SL at 77 K in the energy range of the heavy-hole and light-hole exciton transitions associated with the $n=1$ subbands at various applied biases (electric fields), where the dashed curves indicate the magnified spectra.

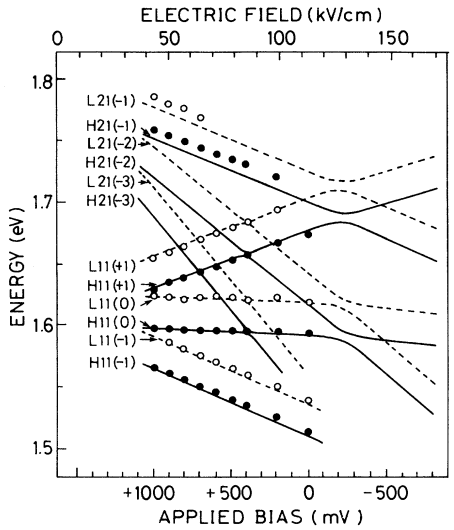

FIG. 2. Calculated and observed Stark-ladder-transition energies of the GaAs(6.4 nm)/AlAs(0.9 nm) SL at 77 K as a function of applied bias (electric field), where the observed energies, indicated by the open and solid circles, are taken from Fig. 1 and our previous report (Ref. 11). The notation $Hn_1n_2(v)$ [$Ln_1n_2(v)$] for the Stark-ladder transition is explained in the text.

transition signals at ~1.595 and ~1.620 eV for the heavy-hole and light-hole excitons, respectively, whereas the ER spectra exhibit six signals labeled *a*-*f*. In the previous work,[11] we have assigned the six ER signals to the following Stark-ladder transitions: *a* and *b* to H11(−1) and L11(−1), *c* and *d* to H11(0) and L11(0), and *e* and *f* to H11(+1) and L11(+1), where the notation of $Hn_1n_2(v)$ [$Ln_1n_2(v)$] indicates the transition with the Stark-ladder index v between the n_1 electron subband and the n_2 heavy-hole (light-hole) subband. The intensities of the Stark-ladder transitions with $v=\pm 1$ remarkably decrease with increasing F, which indicates the enhancement of the wave-function localization.

Figure 2 shows the calculated and observed Stark-ladder-transition energies in the GaAs(6.4 nm)/AlAs(0.9 nm) SL at 77 K as a function of applied bias V_b (electric field F), where the observed energies indicated by open and solid circles are taken from Fig. 1 (the energies of the ER signals indicated by the arrows) and our previous report.[11] Since there is basically no theory to determine the transition energies from the ER signals, the observed energies in Fig. 2 have the inaccuracy corresponding to the ER linewidth, typically 5 meV. In the TM calculation, the GaAs(6.4 nm)/AlAs(0.9 nm) SL is approximated by a system of eleven QW's sandwiched by semi-infinite AlAs layers, and the boundary condition of the Airy functions is identical with that in Ref. 12. The band nonparabolicity for the effective masses is taken into account in accordance with Ref. 13, and the conduction-band-offset ratio is 0.66. The solid (dashed) lines indicate the calculated results for the heavy-hole (light-hole) transitions, which are shifted down by 10 meV to correct the exciton binding energy. It is evident from Fig.2 that the calculated results are consistent with the experimental results of the Stark-ladder transitions and the quantum-confined Stark effect (QCSE) on H11(0) and L11(0). The disagreement, ~9 meV, between the calculated and observed energies of the H21(−1) and L21(−1) transitions seems to be due to the inaccuracy of the calculated energy of the $n=2$ electron subband and/or that of the layer thickness.

Noticing the electric-field range of 120–140 kV/cm in Fig. 2, we find several Stark-ladder transitions exhibiting anticrossing behaviors, H11(0)-H21(−2), L11(0)-L21(−2), H11(+1)-H21(−1), and L11(+1)-L21(−1), which originate from the second-nearest-neighbor resonant coupling between the WS localization state of the $n=1$ electron subband and that of the $n=2$ subband. In addition, the third-nearest-neighbor resonant coupling occurs at ~85 kV/cm, the anticrossing of H11(0)-H21(−3), L11(0)-L21(−3), H11(+1)-H21(−2), and L11(+1)-L21(−2). The anticrossing split is about 8 (3) meV for the second- (third-) nearest-neighbor coupling. It is expected that the anticrossing leads to the appearance of splitting signals of the Stark-ladder transitions.

Figure 3 shows the ER (ΔR) and PC spectra at 77 K in the applied bias (electric field) range of the second-nearest-neighbor resonant coupling between the WS localization states of the $n=1$ and $n=2$ electron subbands. In this electric-field range, the value of eFD (e.g., 88 meV at 120 kV/cm) is about three times larger than the energy width (30 meV) of the $n=1$ electron subband at $F=0$ calculated by using an effective-mass approximation. Hence,

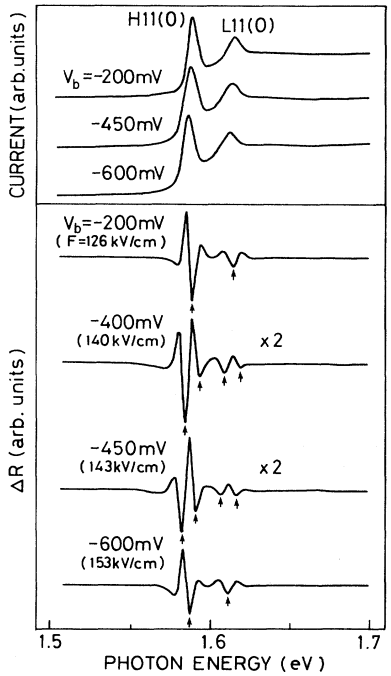

FIG. 3. Electroreflectance and photocurrent spectra at 77 K in the applied bias (electric field) range of the second-nearest-neighbor resonant coupling between the $n=1$ and $n=2$ electron subbands.

the electron wave function is fully localized in individual layers, which results in the disappearance of the Stark-ladder transitions with $v\neq 0$. In Fig. 3 the PC signals of the H11(0) and L11(0) transitions slightly broaden at $V_b=-450$ mV. On the other hand, the ER signals of the H11(0) and L11(0) transitions clearly exhibit splitting line shapes at $V_b=-400$ and -450 mV ($F=140$ and 143 kV/cm). Furthermore, the intensities of the ER signals at $V_b=-400$ and -450 mV are about one-half of those in the nonresonant condition at $V_b=-200$ mV, which indicates the delocalization of the electron wave function resulting from the second-nearest-neighbor resonant coupling.

We discuss the anticrossing behavior of the Stark-ladder transitions caused by the second-nearest-neighbor resonant coupling. Figure 4 shows the observed energies (solid and open circles) of the ER signals for the H11(0) and L11(0) exciton transitions indicated by the arrows in Fig. 3 and the calculated energies (solid and dashed lines) of the H11(0), H21(−2), L11(0), and L21(−2) transitions as a function of applied bias (electric field). The values of V_b (F) for the calculated results are shifted by 160 mV (11 kV/cm) to fit the experimental results. The deviation of V_b (F) is due to the disagreement between the calculated and observed energies of the $n=2$ electron subband (Fig. 2). In Fig. 4 the energies of the splitting ER signals clearly exhibit the anticrossing behavior as a function of V_b (F), and the experimental results agree with the calculated results. The agreement, however, is semiquantitative because we cannot theoretically define the precise transition energies from the ER signals. In addition, the exciton binding energy, which is a 10-meV

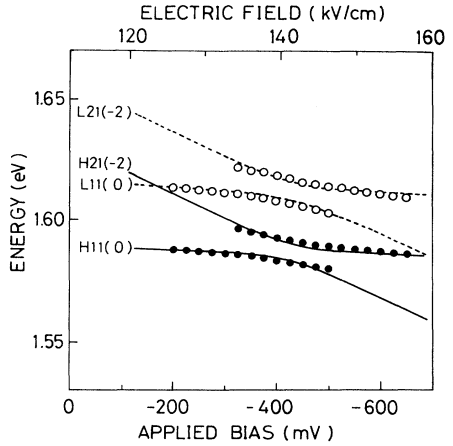

FIG. 4. Energies of the ER signals for the H11(0) and L11(0) exciton transitions indicated by the arrows in Fig. 3 and the calculated energies of the H11(0), H21(−2), L11(0), and L21(−2) transitions as a function of applied bias (electric field) in the second-nearest-neighbor resonant coupling, where the values of the applied bias (electric field) for the calculated results are shifted by 160 mV (11 kV/cm) to fit the experimental results.

correction to the calculated energies in the present work, might be quite sensitive to the delocalization of the wave function at the resonant condition.

Figure 5 shows the ER spectra at 77 K in the applied bias (electric field) range of the third-nearest-neighbor resonant coupling between the WS localization states of the $n=1$ and $n=2$ electron subbands. The calculated results of the H11(0), H21(−3), L11(0), and L21(−3) transitions in Fig. 2 predict that the third-nearest-neighbor resonant coupling occurs at $V_b\simeq+400$ mV

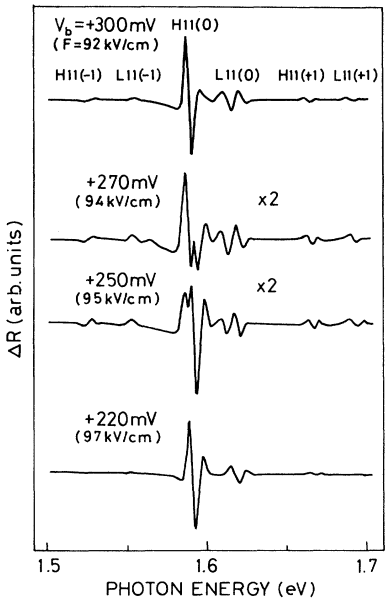

FIG. 5. Electroreflectance spectra at 77 K in the applied bias (electric field) range of the third-nearest-neighbor resonant coupling between the $n=1$ and $n=2$ electron subbands.

($F \simeq 85$ kV/cm). However, it is considered that the real value of F for the resonant coupling is different from the predicted value because of the disagreement between the calculated and observed energies of the $n=2$ electron subband. The real value of F for the third-nearest-neighbor resonant coupling is estimated to be two-thirds of $\simeq 142$ kV/cm at which the second-nearest-neighbor coupling is observed: $F \simeq 95$ kV/cm ($V_b \simeq +250$ mV). In Fig. 5 the ER line shapes of the H11(0) and L11(0) exciton transitions exhibit splitting features at $V_b = +270$ and +250 mV ($F = 94$ and 95 kV/cm), and the intensities are reduced to about one-half of those at $V_b = +300$ and +220 mV ($F = 92$ and 97 kV/cm); the ER properties are similar to those in the second-nearest-neighbor resonant coupling (Fig. 3). Thus, the changes of the ER line shapes in Fig. 5 indicate the third-nearest-neighbor resonant coupling. We note that the PC signals are insensitive to the resonant coupling. The anticrossing split of the third-nearest-neighbor coupling is estimated to be ~ 3 meV from the TM calculation (Fig. 2). The split of the H11(0) signal at $V_b = +270$ and +250 mV in Fig. 5 is almost equal to the expected anticrossing split; however, that of the L11(0) signal, ~ 8 meV, is much larger than the split. The TM calculation suggests that the second-nearest-neighbor coupling between the $n=1$ and $n=2$ light-hole subbands, L11(0)-L12(−2), occurs in this bias range; therefore, the large split of the L11(0) signal may be due to an overlap of the two types of the resonant coupling. The investigation of the light-hole resonant coupling is in progress.

In conclusion, we have detected the second- and third-nearest-neighbor resonant couplings between the WS localization state of the $n=1$ electron subband and that of the $n=2$ subband in the GaAs(6.4 nm)/AlAs(0.9 nm) SL by using ER spectroscopy. It is found that the resonant couplings induce remarkable changes of the ER line shapes of the H11(0) and L11(0) excitons: (1) the appearance of the splitting line shapes due to the anticrossings of the Stark-ladder transitions, H11(0)-H21(−2), L11(0)-L21(−2), H11(0)-H21(−3), and L11(0)-L21(−3); (2) the reduction of the intensities due to the delocalization of the electron wave function. Furthermore, it is demonstrated that ER spectroscopy is much more sensitive to detect the resonant coupling than PC spectroscopy. The experimental results of the resonant coupling obtained by ER spectroscopy are theoretically explained by the TM calculation.

We are grateful to Professor M. Yokota and Professor O. Tanimoto for fruitful discussion of the TM method. We also would like to thank S. Koh for his assistance in the TM calculation and T. Doguchi for his assistance in the measurements.

[1] J. Bleuse G. Bastard, and P. Voisin, Phys. Rev. Lett. **60**, 220 (1988).

[2] E. E. Mendez, F. Agullo-Ruede, and J. M. Hong, Phys. Rev. Lett. **60**, 2426 (1988).

[3] P. Voisin, J. Bleuse, C. Bouche, S. Gaillard, C. Alibert, and A. Regreny, Phys. Rev. Lett. **61**, 1639 (1988).

[4] F. Agullo-Rueda, E. E. Mendez, and J. M. Hong, Phys. Rev. B **38**, 12720 (1988).

[5] I. Bar-Joseph, J. M. Kuo, R. F. Kopf, D. A. B. Miller, and D. S. Chemla, Appl. Phys. Lett. **55**, 340 (1989).

[6] K. Fujiwara, Jpn. J. Appl. Phys. **28**, L1718 (1989).

[7] H. Schneider, K. Fujiwara, H. T. Grahn, K. v. Klitzing, and K. Ploog, Appl. Phys. Lett. **56**, 605 (1990).

[8] B. Soucail, N. Dupuis, R. Ferreira, P. Voisin, A. P. Roth, D. Morris, K. Gibb, and C. Lacelle, Phys. Rev. B **41**, 8568 (1990).

[9] H. Schneider, H. T. Grahn, K. v. Klitzing, and K. Ploog, Phys. Rev. Lett. **65**, 2720 (1990).

[10] A. J. Shields, P. C. Klipstein, M. S. Skolnick, G. W. Smith, and C. R. Whitehouse, Phys. Rev. B **42**, 5879 (1990).

[11] M. Nakayama, I. Tanaka, T. Doguchi, H. Nishimura, K. Kawashima, and K. Fujiwara, Solid State Commun. **77**, 303 (1991).

[12] D. C. Hutchings, Appl. Phys. Lett. **55**, 1082 (1989).

[13] D. F. Nelson, R. C. Miller, C. W. Tu, and S. K. Sputz, Phys. Rev. B **36**, 8063 (1987).